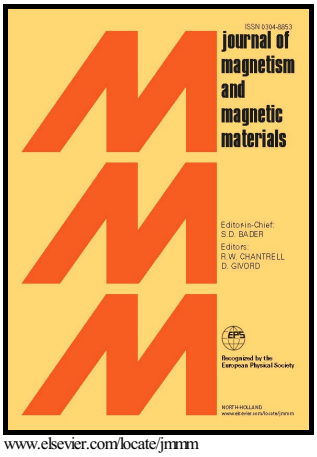

www.elsevier.com/locate/jmmm

Magnetocaloric and magnetic properties of $SmFe_{0.5}mn_{0.5}O_3$ complex perovskite

M.C. Silva-Santana, C.A. daSilva, P. Barrozo, E.J.R. Plaza, L. de los Santos Valladares, N.O. Moreno

PII: S0304-8853(15)30710-1
DOI: http://dx.doi.org/10.1016/j.jmmm.2015.10.076
Reference: MAGMA60769

To appear in: *Journal of Magnetism and Magnetic Materials*

Received date: 19 August 2015
Revised date: 17 October 2015
Accepted date: 20 October 2015

Cite this article as: M.C. Silva-Santana, C.A. daSilva, P. Barrozo, E.J.R. Plaza L. de los Santos Valladares and N.O. Moreno, Magnetocaloric and magnetic properties of $SmFe_{0.5}mn_{0.5}O_3$ complex perovskite, *Journal of Magnetism and Magnetic Materials,* http://dx.doi.org/10.1016/j.jmmm.2015.10.076

Magnetocaloric and magnetic properties of $SmFe_{0.5}Mn_{0.5}O_3$ complex perovskite

M. C. Silva-Santana[a], C. A. daSilva[a], P. Barrozo[a], E. J. R. Plaza[a], L. de los Santos Valladares[b,c], N. O. Moreno[a,*]

[a] *Departamento de Física, Universidade Federal de Sergipe, 49100-000, São Cristóvão, SE, Brazil*
[b] *Cavendish Laboratory, Department of Physics, University of Cambridge, J.J. Thomson Ave., Cambridge CB3 0HE, United Kingdom.*
[c] *Laboratorio de Cerámicos y Nanomateriales, Facultad de Ciencias Física, Universidad Nacional Mayor de San Marcos, Ap. Postal 14-0149, Lima, Peru.*

Abstract

In this paper, we have investigated the physical properties of $SmFe_{0.5}Mn_{0.5}O_3$ complex perovskite samples, synthesized by means of combustion reaction method. X-ray powder diffraction indicates the formation of single phase perovskite with orthorhombic structure. Low magnetic field measurements shows remarkable transition at 234 K related to spin reorientation. The magnetocaloric effect shows two peaks related to magnetic behavior changes, at 18 K and at 234 K. The transition about 234 K presents inverse magnetocaloric effect. The entropy variation from magnetocaloric effect shows power law as function of applied magnetic field with maximum entropy change 5.6 J/kg K with field variation of 70 kOe. Critical exponents extracted from ΔS vs. H presents a remarkable sharp peak near antiferromagnetic to weak ferromagnetic transition temperature.

Keywords:
Complex Perovskites; Magnetic Properties; Combustion Synthesis; Spin Reorientation; Magnetocaloric Effect; Inverse Magnetocaloric Effect
PACS: 71.27.+a, 75.30.Sg, 75.47.Lx, 81.20.Ka

1. Introduction

Complex metal oxides such as manganites and orthoferrites are interesting because their rich set of compounds, properties and structures. During the last decades, system-

*Corresponding author
Email address: nomoreno@ufs.br (N. O. Moreno)

atic studies on manganites containing rare earth and alkali earth ions have shown that these systems possess a wide range of physical phenomena including multiferroicity, colossal magnetocapacitance and colossal magnetoresistance [1, 2, 3].

Studies carried out in orthoferrites indicate that these compounds have Néel temperature between 620 K and 740 K.[4] Due to the anisotropy effects associated with rare earth and Fe^{3+} magnetic interactions, this family of compounds exhibits spin reorientation.[5] The spin reorientation in orthoferrites commonly is processed by switching from Γ_4 canted antiferromagnetic reducible representation to the Γ_2 antiferromagnetic ordering.[6, 7] The known exception is $DyFeO_3$ which spin reorientation is performed from Γ_4, at high temperature, to Γ_1, a coplanar antiferromagnetic phase [8, 9].

Systems possessing multiples magnetic phases present interesting entropy variation as function of temperature and magnetic field, mainly close to the magnetic transition temperature, exhibiting magnetocaloric effect [10, 11].

The magnetocaloric effect can be defined as the thermal response of magnetic materials due to changes of applied magnetic field. [12, 13, 14] Its discovery in metals along with the adiabatic cooling, proposed by Debye and Giauque, promoted the magnetocaloric effect (MCE) as a mean of reaching low temperatures [15, 16, 17, 18]. However, this effect is not only important in applications such as magnetic refrigeration, but it is also an useful tool for fundamental physics because it can hint on the nature of magnetic phases and transitions [19, 20, 21, 22].

Taking into account the usefulness of magnetocaloric, a study conducted on $SmMnO_3$ perovskite indicated the presence of magnetocaloric effect with maximum entropy change 8 J/kgK for an applied field variation of 0-70 kOe at transition temperature.[23] Investigations have also been directed to study magnetocaloric effect in more complex perovskites such as the ordered perovskite $Ba_2Fe_{1-x}Cr_xMoO_6$, $Ba_2Fe_{1+x}Mo_{1-x}O_6$ and $Sr_2FeMo_{1-x}W_xO_6$ [24, 25, 26].

Single crystals of $DyMn_{0.5}Co_{0.5}O_3$ and $La_{0.6}Pr_{0.1}Ca_{0.3}MnO_3$ disordered perovskite have MCE value as compared to that for Gd [27, 28].

In this work, we investigate the magnetic behavior of complex perovskite $SmFe_{0.5}Mn_{0.5}O_3$ synthesized by combustion reaction, and its behavior in terms of magnetocaloric effect at various intensities of magnetic field variation.

2. Experimental Details

2.1. Sample Preparation

Polycrystalline $SmFe_{0.5}Mn_{0.5}O_3$ samples were produced by the combustion reaction method.[29] A solution containing the stoichiometric quantity of high quality grade reagents $Sm(NO_3)_3.6H_2O$ (Aldrich 99.98%), $MnCl_2{:}4H_2O$ (Aldrich 99%) and $Fe(NO_3)_3.9H_2O$ (Aldrich; 99.9%) was formed by diluting them in distilled water. The solution was subjected to vigorous stirring with a magnetic stirrer at temperature about 120°C

for one hour in order to remove water excess. During the stirring and evaporation process a stoichiometric amount of urea organic fuel, calculated according to propellants chemistry, was added [30].

After removal of most of water, the formation process of a sol-gel takes place. The backer containing the sol-gel is placed on a hot plate with temperatures above 300°C for few minutes in order to start the spontaneous combustion reaction with intense flame and expressive output of gas.

The resulting product is a sponge containing very fine powder. The product obtained from the combustion reaction is ground in agate mortar and then subjected to a heat treatment at 1300°C for 12 h in air atmosphere.

2.2. Experimental Apparatus

The crystal structure of samples, as well as its purity were analyzed by using a Rigaku Inc. X-ray diffractometer with Cu Kα radiation and Bragg-Bretano geometry. X-ray diffraction data were collected in the range $20° - 80°$ in steps of 0.02° at room temperature. Magnetic measurements using fields up to 7 T, in the range 2 K - 400 K, were performed in a commercial Quantum Design MPMS Evercool 7 T magnetometer with SQUID sensor.

2.3. Magnetocaloric Effect Calculations

The magnetocaloric effect can be obtained indirectly from a set of magnetic measurements as a function of temperature and magnetic field. The magnetic entropy variation due to the magnetic field application can be calculated through the well-known integral which follows from the differential Maxwell thermodynamic relations, expressed in the equation (1) [14, 24]:

$$\Delta S_M(T,H) = \int_0^H \left(\frac{\partial M}{\partial T}\right)_H dH' \qquad (1)$$

The expression of equation (1) can be discretized in order to be used with experimental magnetization isothermal data. The entropy variation can be calculated from experimental data according the expression [24]:

$$-\Delta S_M = \sum_i \frac{M_i - M_{i+1}}{T_{i+1} - T_i}\Delta H \qquad (2)$$

where M_{i+1} and M_i are the magnetization values measured at magnetic field H and at temperatures T_{i+1}, T_i, respectively.

3. Results and discussion

X-ray diffraction (XRD) measurements carried out at room temperature showed the formation of single phased $SmFe_{0.5}Mn_{0.5}O_3$ sample without indication of impurity phases at least in the sensitivity range of our experimental apparatus. The diffraction peaks have been easily indexed according to structure belonging to the orthorhombic *Pbnm* (62) space group. The indexed peaks were compatible with the diffraction pattern cataloged in the crystallographic database under ICSD 27279 [31].

Through the Rietveld refinement, the lattice parameters have been estimated using

the Topas software [32]. The parameters values obtained from refinement with $GoF = 1.22$, are listed in Table 1. Fig. 1 shows the x-ray diffraction pattern of $SmFe_{0.5}Mn_{0.5}O_3$ powder sample taken at room temperature. The inset shows the main peak profile and its fit quality.

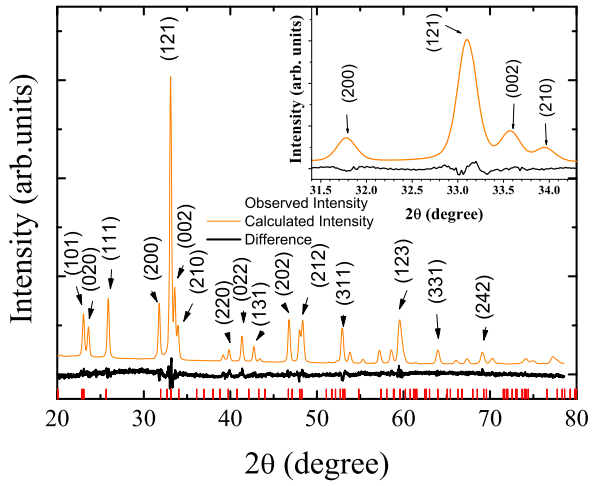

Figure 1: X-ray diffraction pattern for $SmFe_{0.5}Mn_{0.5}O_3$ at room temperature. The open circles represent the observed patterns; continuous lines represent calculated and difference patterns. The tick marks correspond to the position of the allowed Bragg reflections. The inset shows the main peaks profile.

Table 1: The Rietveld refinement parameters of orthorhombic $SmFe_{0.5}Mn_{0.5}O_3$ ($Pbnm$) with $a = 5.3615$(Å), $b = 5.6253$(Å) and $c = 7.5189$(Å) at $T = 293$ K obtained by the combustion method.

Atom	Wyc.	x/a	y/b	z/c	Occ.
Sm1	4c	0.9802(8)	0.0662(2)	0.25	1.0
Fe1	4b	0.0	0.5	0.0	0.5
Mn1	4b	0.0	0.5	0.0	0.5
O1	4c	0.0945(2)	0.4033(7)	0.25	1.0
O2	8d	0.6702(0)	0.3137(0)	0.0582(4)	1.0

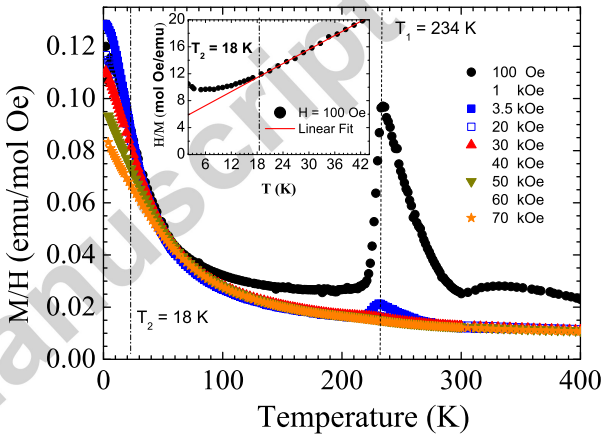

Figure 2: M/H as a function of temperature for magnetic fields in the range of 100 Oe and 70 kOe. The inset shows the low-T data of H/M vs. T. The solid line is a fit to Curie-Weiss law.

The magnetic behavior of the $SmFe_{0.5}Mn_{0.5}O_3$ can be seen in the M/H vs. temperature curves for various magnetic fields as shown in Fig. 2.

The magnetization has strong field dependence in all range of temperature resulting in different shapes of curves. The magnetization can be described in three different parts according to its behavior.

At high temperatures, from 300 K up to 400 K, the M/H curves present small non overlapping behavior probably related to reminiscent short-range magnetic interaction near to Néel transition.

Below 300 K, the system experiences a magnetic ordering with a increasing of magnetization up to 234 K where an abrupt re-

duction is observed. The peak formed in this range of temperature is better visualized with low magnetic field measurements.

For smaller temperatures, down to 18 K, the magnetization intensify itself forming a paramagnetic like tail with intensity rise associated to the magnetic contribution provided by the Sm^{3+} ions. This type of magnetic contribution is often found in perovskites containing magnetic rare earth ions [23, 33]. Below 18 K, the magnetization deviates from paramagnetic behavior as shows the inset of Fig. 2.

The magnetization behavior on such systems can be understood taking into account different interactions involving Fe^{3+}, Mn^{3+} and Sm^{3+} ions. It is known that the $SmFeO_3$ transits from paramagnetic (PM) to weak-feromagnetic (WFM) at 670 K. The WFM phase is followed by a spin reorientation switching from [001] to easy axis [100] direction at temperatures below 480 K [34, 35, 36, 37].

The formation of the perovskites containing Fe^{3+} and Mn^{3+} in the center of octahedra induces additional complexity, mainly resultant from the intricate interactions between the sublattices, Jahn-Teller activity of Mn^{3+}, single ion anisotropy etc. [38].

The substitution of Fe^{3+} ($S = 5/2$) by Mn^{3+} ($S = 2$) weakens the Fe^{3+}–Fe^{3+} interaction, reducing the critical temperature [38]. Other effect of Mn^{3+} presence is the increasing of temperature of WFM–AFM spin reorientation. The Mn^{3+} content promotes changes in environment, mainly in the effective anisotropy resulting to shift of spin reorientation to higher temperatures. Such effects: the increasing of spin reorientation and decreasing of Néel temperature were also observed in $SmFe_{1-x}Mn_xO_3$ $x = 0.0 - 0.3$ samples [39]. Similar results have been obtained by researches on isomorphic $DyFe_{1-x}Mn_xO_3$ [33]. In fact, $DyFe_{1-x}Mn_xO_3$ have similar magnetic behavior containing PM – WFM and WFM – AFM transitions. Similarly, the increasing Mn content leads to decrease the PM – WFM transition temperature whereas the spin reorientation temperature increases [33, 38].

Below the temperature of spin reorientation (T_{SR}), it is known that the principal contribution to the magnetization of the orthoferrites comes from the rare-earth ions [40]. Commonly, the magnetic long-range order of rare earth ions in orthoferrites is established at low temperature (close liquid-helium temperature). However, in $SmFeO_3$ there is evidence of magnetic coupling between Sm^{3+} and the canted spin Fe^{3+} at $T < T_{SR} = 480$ K [34, 41, 42, 43]. In this situation, the magnetic moment of Sm^{3+} forms an antiparallel order with the canted spin resultant from the Fe^{3+} sublattice. However, it is known that the rare earth can also form an parallel arrange with weak ferromagnetic component [5]. Based on the arguments mentioned above, we suggest that deviation from paramagnetic-like behavior observed at 18 K (see the inset of Fig. 2) may be related to a consequence of the interplay between Sm-4f and (Fe, Mn)-3d electrons [44, 45, 46].

The magnetization behavior as a function of magnetic field for some temperatures is shown in the Fig. 3.

At 2 K, the magnetization shows nonlin-

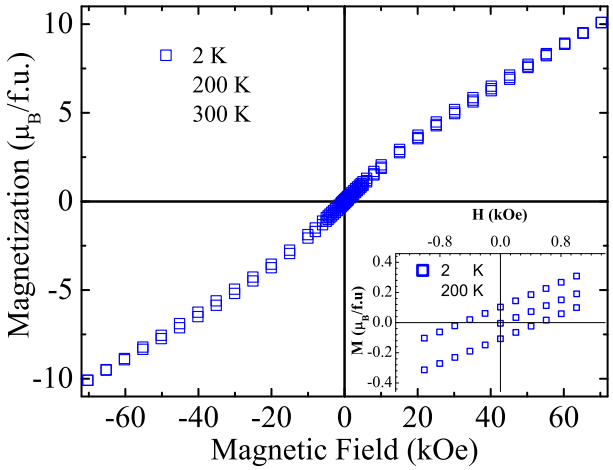

Figure 3: Magnetization as a function of applied magnetic field for $SmFe_{0.5}Mn_{0.5}O_3$ obtained at 2 K, 200 K and 300 K. The inset shows the low-field behavior at 2 K and 200 K.

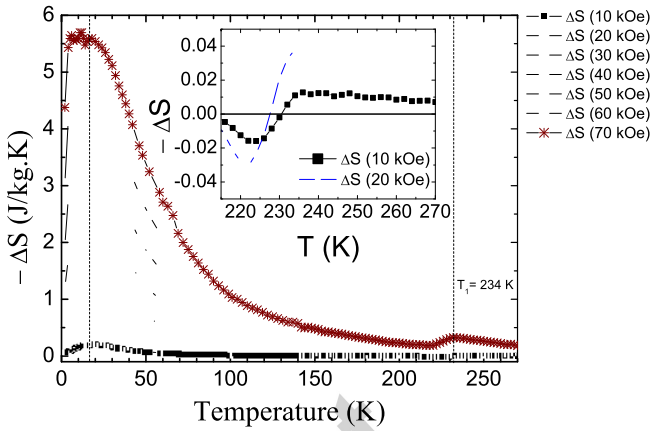

Figure 4: Magnetocaloric effect as a function of temperature and magnetic field for $SmFe_{0.5}Mn_{0.5}O_3$. The inset shows presence of inverse magnetocaloric effect close to AFM-WFM transition.

ear behavior with irreversibility in the low field range presenting remanent magnetization $Mr \simeq 0.10\mu_B/f.u.$ Extracting the paramagnetic contribution, the saturation of magnetization was estimated with value $Ms \simeq 0.70\mu_B/f.u.$ These small values of remanent magnetization and saturation suggest the existence of weak ferromagnetic component even at low temperature. Measurement taken at 200 K, just below the abrupt WFM – AFM transition, presents a linear magnetic behavior as a function of the magnetic field without irreversibility. The curve taken at 200 K can be visualized in the inset of Fig. 3. This behavior is compatible with AFM ordering type.

The magnetocaloric effect curves, obtained according procedure explained elsewhere[24], are plotted as a function of temperature and magnetic field as shows the Fig. 4.

The change of magnetic entropy increases for high variation of applied field. This behavior is expected since higher magnetic fields easily align the magnetic moments, thus reducing the entropy.

About 234 K, a small asymmetric peak is observed. This peak is associated to effect on entropy from AFM – WFM transition. The inset in the Fig. 4 shows the details variation of entropy in the range of temperature in which the AFM – WFM transition occurs. This transition leads to the presence of inverse magnetocaloric effect (IMCE) characterized by the depression centered in 222 K. The depression, shown in the inset of Fig. 4 increases with applied field, until a critical field is reached and the IMCE is suppressed. Some Ca, Sr doped $LaMnO_3$ samples present similar IMCE, and it is often associated to

the stabilization of antiferromagnetic order [47, 48]. The entropy variation curves for our sample are close compatible to the curves obtained theoretically by von Ranke *et al.*, on antiferromagnetic type transition [49].

Below 220 K, $-\Delta S$ increases up to a maximum variation of 5.6 J/kg K at 18 K. The peak about 18 K indicates that the system may be experiencing changes in magnetic configuration. The value of entropy change for ΔH =10 kOe is rather small (0.2 J/kg K) specially in comparison to magnetocaloric effect observed in other Sm based perovskites such as $Sm_{0.52}Sr_{0.48}MnO_3$ that possesses 5.9 J/kg K for ΔH=10 kOe and $Nd_{0.6}La_{0.1}Sr_{0.4}MnO_3$ that exhibits 3.14 J/kg K for ΔH=15 kOe [50, 51]. In fact, $Sm_{0.52}Sr_{0.48}MnO_3$ have been reported as presenting higher magnetocaloric effect in comparison to others known rare earth based perovskite oxides.

The value of magnetocaloric effect of our sample is in the same order in comparison to manganites samples as $La_{0.9}Pb_{0.1}MnO_3$ for 10 kOe of magnetic variation [52, 53]. The intensity variation of entropy is generally related to the magnetic field as power law according the equation (3) [54, 55];

$$|\Delta S| = aH^n, \tag{3}$$

where a, and n are normalization constant and power exponent respectively.

For magnetic systems with single magnetic transition, mean field calculation states that the exponent n varies with temperature, reaching values close to 1.0 for low temperatures (far from transition temperature), 2/3 at the critical temperature and 2.0 for paramagnetic temperatures [54].

It was also found that our $SmMn_{0.5}Fe_{0.5}O_3$ sample presents power law for all $|\Delta S|$ vs. H curves at temperatures in the range of 2 K - 270 K. Fig. 5 shows the behavior of magnetocaloric effect in relation to the magnetic field. It can be easily adjusted to fit a power law. This behavior is found in several measurements at different temperatures. The monotonic increasing of entropy variation as a function of magnetic field presents smaller exponent at 18 K with value about $n \simeq 1.5$. This temperature is coincident with the maximum of second peak on entropy variation seen in the Fig. 4.

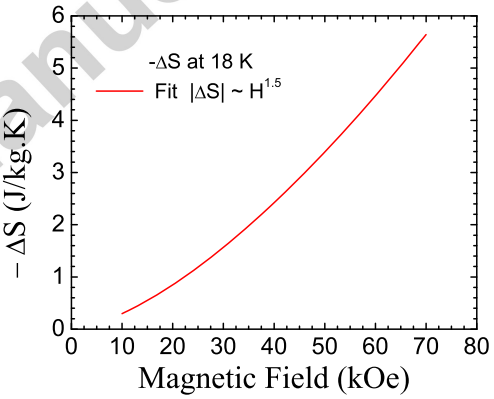

Figure 5: Variation of entropy as a function of magnetic field at T = 18 K. The solid line is the fitted curve by a power law.

We noted that the exponent n as a function of temperature, shown in the Fig. 6, presents different values in comparison to those estimated by mean field [54]. This result is not

surprising because our system present multiples magnetic transitions and interactions that are not well modeled by mean field theory.

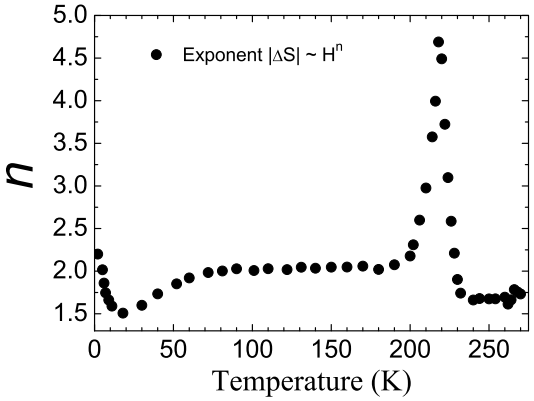

Figure 6: Power law exponent as a function of temperature for $SmFe_{0.5}Fe_{0.5}O_3$.

At $T = 2$ K, the exponent is close to 2.2. Increasing temperature, the exponent decreases finding its minimum at 18 K with $n \simeq 1.5$. This temperature is coincident with change of slope observed in H/M (see Fig. 2). Above 18 K, the exponent increases remaining constant with $n \simeq 2$ up to 180 K. At higher temperatures, the exponent has a strong anomaly peak at 218 K with $n \simeq 4.6$ in the same range that occurs IMCE (see Fig.4). From 240 K up to 270 K, the exponent stabilizes with $n \simeq 1.66$.

The exponent values for some manganites are well behaved in comparison to the exponent estimated for our sample. In a manganite, for example, the value of exponent is $n \simeq 2.0$ changing effectively only in measurement with high magnetic fields [56]. The values of exponent for our sample differs from this behavior due to $SmFe_{0.5}Mn_{0.5}O_3$ multiple transition and nature of interactions.

High field measurements indicate that the entropy variation at 18 K increases proportionally to the field not presenting any trend to exhaustion even for high field as 70 kOe. This fact can be related to contribution from rare earth ion [57].

4. Conclusions

Polycrystalline $SmFe_{0.5}Mn_{0.5}O_3$ sample was successfully synthesized by the combustion synthesis method. X-ray diffraction measurements indicate formation of pure phase sample with orthorhombic symmetry. Magnetization vs. temperature measurements in the range 2 K-400 K have two magnetic transitions: one at 234 K related to WFM – AFM spin reorientation and another at low temperature related to the interplay Sm-4f and Fe, Mn-3d electrons. At higher fields, the peak at 234 K is virtually suppressed suggesting elastic processes. Magnetocaloric effect curves were obtained from various measurements of the magnetization as a function of temperature and magnetic field. The magnetocaloric effect presents two peaks related to magnetic transitions and events at 18 K and 234 K. AFM – WFM transition at 234 K leads to inverse magnetocaloric effect with fingerprint depression centered at 222 K.

At low temperature, the magnetization is influenced mainly by the contribution of Sm effecting Mn, Fe sublattices, while at high temperature the main contribution is related

to ions in B –site at the time that Sm behaves paramagnetically. The Sm presence induces the spin reorientation.

The variation of entropy scales as power law as function of magnetic field. However, variation of entropy power law presents unusual exponent values as function of temperature with remarkable sharp peak near AFM – WFM spin reorientation transition temperature.

Acknowledgments

M. C. Silva-Santana and N. O. Moreno are grateful for the partial support provided by CAPES (PDSE grant number BEX 14354/13-6), CNPq and FAPITEC/SE.

[1] C. R. Serrao, A. Sundaresan, C. N. R. Rao, Multiferroic nature of charge-ordered rare earth manganites, J. Phys. Condens. Matter 19 (49) (2007) 496217.

[2] T. Goto, T. Kimura, G. Lawes, A. P. Ramirez, Y. Tokura, Ferroelectricity and giant magnetocapacitance in perovskite rare-earth manganites, Phys. Rev. Lett. 92 (25) (2004) 257201.

[3] T. V. Ramakrishnan, Modelling colossal magnetoresistance manganites, J. Phys. Condens. Matter 19 (12) (2007) 125211.

[4] S. Parida, S. Rakshit, Z. Singh, Heat capacities, order–disorder transitions, and thermodynamic properties of rare-earth orthoferrites and rare-earth iron garnets, J. Solid State Chem. 181 (1) (2008) 101–121.

[5] T. Yamaguchi, Theory of spin reorientation in rare-earth orthochromites and orthoferrites, J. Phys. Chem. Solids 35 (4) (1974) 479–500.

[6] K. P. Belov, A. K. Zvezdin, A. M. Kadomtseva, Rare-earth orthoferrites, symmetry and non-heisenberg exchange, Soviet Scientific Reviews, Section A: Physics Reviews, Edited by I. M. Khalatnikov 9 (1987) 117–222.

[7] L. Tsymbal, Y. B. Bazaliy, V. Derkachenko, V. Kamenev, G. Kakazei, F. Palomares, P. Wigen, Magnetic and structural properties of spin-reorientation transitions in orthoferrites, J. Appl. Phys. 101 (12) (2007) 123919.

[8] G. Gorodetsky, L. M. Levinson, Direct observation of reorientation of antiferromagnetic axis in $DyFeO_3$, Phys. Lett. A 31 (1970) 115–116.

[9] X. Fu, X. Liu, J. Zhou, Terahertz spectroscopic observation of spin reorientation induced antiferromagnetic mode softening in $DyFeO_3$ ceramics, Mater. Lett. 132 (2014) 190–192.

[10] P. Mandal, C. Serrao, E. Suard, V. Caignaert, B. Raveau, A. Sundaresan, C. Rao, Spin reorientation and magnetization reversal in the perovskite oxides, $YFe_{1-x}Mn_xO_3$($0 \leq x \leq 0.45$): A neutron diffraction study, J. Solid State Chem. 197 (2013) 408–413.

[11] M. Shao, S. Cao, Y. Wang, S. Yuan, B. Kang, J. Zhang, Large magnetocaloric effect in $HoFeO_3$ single crystal, Solid State Commun. 152 (11) (2012) 947–950.

[12] K. A. Gschneidner, V. K. Pecharsky, Magnetocaloric materials, Annu. Rev. Mater. Sci. 30 (2000) 387–429.

[13] A. M. Tishin, Y. I. Spichkin, The magnetocaloric effect and its applications, CRC Press, 2003.

[14] K. A. Gschneidner, V. K. Pecharsky, A. O. Tsokol, Recent developments in magnetocaloric materials, Rep. Prog. Phys. 68 (6) (2005) 1479.

[15] E. Warburg, Magnetische untersuchungen: ber einige wirkungen der corcitivkraft, Ann. der Phys. 13 (1881) (1881) 141–164.

[16] P. Debye, Einige bemerkungen zur magnetisierung bei tiefer temperatur, Annalen der Physik 386 (25) (1926) 1154–1160.

[17] A. Rowe, A. Tura, Experimental investigation of a three-material layered active magnetic regenerator, Int. J. Refrigeration 29 (8) (2006) 1286 – 1293.

[18] K. G. Sandeman, Magnetocaloric materials: The search for new systems, Scripta Materialia 67 (6) (2012) 566 – 571.

[19] O. Tegus, E. Brück, L. Zhang, K. Buschow, F. De Boer, et al., Magnetic-phase transitions and magnetocaloric effects, Physica B 319 (1) (2002) 174–192.

[20] V. Franco, J. Blázquez, A. Conde, Field dependence of the magnetocaloric effect in materials with a second order phase transition: A master curve for the magnetic entropy change, Appl. Phys. Lett. 89 (22) (2006) 222512–222512.

[21] V. Franco, A. Conde, J. Romero-Enrique, J. Blázquez, A universal curve for the magnetocaloric effect: an analysis based on scaling relations, J. Phys. Condens. Matter 20 (28) (2008) 285207.

[22] V. Franco, A. Conde, Scaling laws for the magnetocaloric effect in second order phase transitions: From physics to applications for the characterization of materials, Int. J. Refrigeration 33 (3) (2010) 465–473.

[23] C. A. daSilva, R. S. Silva, E. J. R. Plaza, N. O. Moreno, Magnetic state and magnetocaloric effect of $SmMnO_3$, J. Supercond. Nov. Magn. 26 (7) (2013) 2497–2499.

[24] M. El-Hagary, Effect of partial substitution of Cr^{3+} for Fe^{3+} on magnetism, magnetocaloric effect and transport properties of Ba_2FeMoO_6 double perovskites, J. Alloys Compd. 502 (2) (2010) 376 – 381.

[25] W. Zhong, W. Liu, X. Wu, N. Tang, W. Chen, C. Au, Y. Du, Magnetocaloric effect in the ordered double perovskite

$Sr_2FeMo_{1-x}W_xO_6$, Solid State Commun. 132 (34) (2004) 157 – 162.

[26] W. Zhong, N. J. Tang, X. L. Wu, W. Liu, W. Chen, H. Y. Jiang, Y. W. Du, Magnetocaloric effect above room temperature in the ordered double-perovskite $Ba_2Fe_{1+x}Mo_{1-x}O_6$, J. Magn. Magn. Mater. 282 (0) (2004) 151 – 155.

[27] C. Ganeshraj, R. Pradheesh, P. Santhosh, Structural, magnetic, transport and magnetocaloric properties of metamagnetic $DyMn_{0.5}Co_{0.5}O_3$, J. Appl. Phys. 111 (7) (2012) 07A914.

[28] N. Bebenin, R. Zainullina, V. Ustinov, Y. Mukovskii, Effect of inhomogeneity on magnetic, magnetocaloric, and magnetotransport properties of $La_{0.6}Pr_{0.1}Ca_{0.3}MnO_3$ single crystal, J. Magn. Magn. Mater. 324 (6) (2012) 1112 – 1116.

[29] X. Qi, J. Zhou, Z. Yue, Z. Gui, G. Li, Auto-combustion synthesis of nanocrystalline $LaFeO_3$, Materials Chemistry and Physics 78 (1) (2003) 25 – 29.

[30] S. Jain, K. Adiga, V. Pai Verneker, A new approach to thermochemical calculations of condensed fuel-oxidizer mixtures, Combustion and Flame 40 (0) (1981) 71 – 79.

[31] M. Marezio, J. Remeika, P. Dernier, The crystal chemistry of the rare earth orthoferrites, Acta Crystallogr. Sec. B 26 (12) (1970) 2008–2022.

[32] A. Bruker, Topas v3: General profile and structure analysis software for powder diffraction data, Users Manual, Bruker AXS, Karlsruhe, Germany.

[33] F.-K. Chiang, M.-W. Chu, F. C. Chou, H. T. Jeng, H. S. Sheu, F. R. Chen, C. H. Chen, Effect of jahn-teller distortion on magnetic ordering in $Dy(Fe,Mn)O_3$ perovskites, Phys. Rev. B 83 (24) (2011) 245105.

[34] J.-H. Lee, Y. K. Jeong, J. H. Park, M.-A. Oak, H. M. Jang, J. Y. Son, J. F. Scott, Spin-canting-induced improper ferroelectricity and spontaneous magnetization reversal in $SmFeO_3$, Phys. Rev. Lett. 107 (11) (2011) 117201.

[35] R. L. White, Review of recent work on the magnetic and spectroscopic properties of the rare–earth orthoferrites, J. Appl. Phys. 40 (3) (1969) 1061–1069.

[36] R. M. Bozorth, H. J. Williams, D. E. Walsh, Magnetic properties of some orthoferrites and cyanides at low temperatures, Phys. Rev. 103 (3) (1956) 572–578.

[37] Z. Zhou, L. Guo, H. Yang, Q. Liu, F. Ye, Hydrothermal synthesis and magnetic properties of multiferroic rare-earth orthoferrites, J. Alloys Compd. 583 (2014) 21 – 31.

[38] F. Hong, Z. Cheng, H. Zhao, H. Kimura, X. Wang, Continuously tunable magnetic phase transitions in the

$DyMn_{1-x}Fe_xO_3$ system, Appl. Phys. Lett. 99 (9) (2011) 092502.

[39] K. Bouziane, A. Yousif, I. A. Abdel-Latif, K. Hricovini, C. Richter, Electronic and magnetic properties of $SmFe_{1-x}Mn_xO_3$ orthoferrites (x=0.1, 0.2, and 0.3), J. Appl. Phys. 97 (10) (2005) 1–3.

[40] S. J. Yuan, W. Ren, F. Hong, Y. B. Wang, J. C. Zhang, L. Bellaiche, S. X. Cao, G. Cao, Spin switching and magnetization reversal in single-crystal $NdFeO_3$, Phys. Rev. B 87 (18) (2013) 184405.

[41] Y. K. Jeong, J.-H. Lee, S.-J. Ahn, H. M. Jang, Temperature-induced magnetization reversal and ultra-fast magnetic switch at low field in $SmFeO_3$, Solid State Commun. 152 (13) (2012) 1112–1115.

[42] L. G. Marshall, J.-G. Cheng, J.-S. Zhou, J. B. Goodenough, J.-Q. Yan, D. G. Mandrus, Magnetic coupling between Sm^{3+} and the canted spin in an antiferromagnetic $SmFeO_3$ single crystal, Phys. Rev. B 86 (2012) 064417.

[43] S. Cao, H. Zhao, B. Kang, J. Zhang, W. Ren, Temperature induced spin switching in $SmFeO_3$ single crystal, Scientific reports 4.

[44] H. Zhao, S. Cao, R. Huang, W. Ren, S. Yuan, B. Kang, B. Lu, J. Zhang, Enhanced 4f-3d interaction by ti-doping on the magnetic properties of perovskite $SmFe_{1-x}Ti_xO_3$, J. Appl. Phys. 114 (11) (2013) 113907.

[45] J.-G. Cheng, J.-S. Zhou, J. Goodenough, Y. Su, Y. Sui, Y. Ren, Exchange field on the rare earth Sm^{3+} in a single crystal perovskite $smmno_3$, Phys. Rev. B. 84 (10) (2011) 104415.

[46] J.-S. Jung, A. Iyama, H. Nakamura, M. Mizumaki, N. Kawamura, Y. Wakabayashi, T. Kimura, Magnetocapacitive effects in the néel n-type ferrimagnet $SmMnO_3$, Physical Review B 82 (21) (2010) 212403.

[47] A. Biswas, S. Chandra, T. Samanta, B. Ghosh, S. Datta, M. H. Phan, A. K. Raychaudhuri, I. Das, H. Srikanth, Universality in the entropy change for the inverse magnetocaloric effect, Phys. Rev. B 87 (13) (2013) 134420.

[48] S. Chandra, A. Biswas, S. Datta, B. Ghosh, A. Raychaudhuri, M. Phan, H. Srikanth, Multiple magnetic transitions and magnetocaloric effect in hydrothermally synthesized single crystalline $La_{0.5}Sr_{0.5}MnO_3$ nanowires, in: Symposium HH Nanocomposites, Nanostructures and Heterostructures of Correlated Oxide Systems, Vol. 1454 of MRS Proceedings, 2012, pp. 63–68.

[49] P. J. von Ranke, N. A. de Oliveira, B. P. Alho, E. J. R. Plaza, V. S. R. de Sousa, L. Caron, M. . S. Reis, Understanding the inverse magnetocaloric

effect in antiferro- and ferrimagnetic arrangements, J. Phys. Condens. Matter 21 (5) (2009) 056004.

[50] P. Sarkar, P. Mandal, P. Choudhury, Large magnetocaloric effect in $Sm_{0.52}Sr_{0.48}MnO_3$ in low magnetic field, Appl. Phys. Lett. 92 (18) (2008) –.

[51] J. Fan, L. Ling, B. Hong, L. Pi, Y. Zhang, Magnetocaloric effect in perovskite manganite, J. Magn. Magn. Mater. 321 (18) (2009) 2838 – 2841.

[52] S.-G. Min, K. S. Kim, S. C. Yu, H. S. Suh, S. W. Lee, Magnetocaloric properties of $La_{1-x}Pb_xMnO_3$ (x = 0.1, 0.2, 0.3) compounds, in: Magnetics Conference, 2005. INTERMAG Asia 2005. Digests of the IEEE International, 2005, pp. 1481–1482.

[53] M.-H. Phan, S.-Y. Seong-Cho Yu, Review of the magnetocaloric effect in manganite materials, J. Magn. Magn. Mater. 308 (2) (2007) 325 – 340.

[54] H. Oesterreicher, F. T. Parker, Magnetic cooling near curie temperatures above 300 k, J. Appl. Phys. 55 (12) (1984) 4334–4338.

[55] V. Franco, A. Conde, Scaling laws for the magnetocaloric effect in second order phase transitions: From physics to applications for the characterization of materials, Int. J. Refrigeration 33 (3) (2010) 465–473.

[56] A. Biswas, S. Chandra, T. Samanta, M. Phan, I. Das, H. Srikanth, The universal behavior of inverse magnetocaloric effect in antiferromagnetic materials, J. Appl. Phys. 113 (17) (2013) 17A902–17A902–3. doi:10.1063/1.4793768.

[57] Y. Sun, W. Tong, N. Liu, Y. Zhang, Magnetocaloric effect in polycrystalline $(La_{0.5}Gd_{0.2})Sr_{0.3}MnO_3$, J. Magn. Magn. Mater. 238 (1) (2002) 25 – 28.